



# A novel modeling approach of aluminum foam based on MATLAB image processing



Xiaolei Zhu <sup>a,\*</sup>, Shigang Ai <sup>b</sup>, Daining Fang <sup>b</sup>, Bin Liu <sup>a</sup>, Xiaofeng Lu <sup>c</sup>

<sup>a</sup> AML, Department of Engineering Mechanics, Tsinghua University, Beijing 100084, China

<sup>b</sup> State Key Laboratory of Turbulence and Complex System, College of Engineering, Peking University, Beijing 100871, China

<sup>c</sup> Department of Mechanical Engineering, Nanjing University of Technology, Nanjing, Jiangsu Province 211816, China

## ARTICLE INFO

### Article history:

Received 23 July 2013

Received in revised form 17 September 2013

Accepted 13 October 2013

Available online 12 November 2013

### Keywords:

Aluminum foam

Image processing

Finite element model

MATLAB

Compression

## ABSTRACT

Metal foams are a relatively new class of materials exhibiting well physical and mechanical properties which make them attractive in a number of engineering applications. In this paper, a novel modeling approach is proposed to establish the finite element model (FEM) of aluminum foam. Firstly, MATLAB image processing is used to deal with synchrotron X-ray computed tomography ( $\mu$ CT) scanning images of real aluminum foam and reconstruct geometric model. Secondly, two-step mesh method is employed to mesh the geometrical model by appropriate selection of node, and then establish the FEM of aluminum foam directly. This approach is used to calculate the compression performance of aluminum foam based on ABAQUS, of which porosity is set as 56.41%, 56.71% and 58.02%, respectively, and the matrix material is ZL102. The calculation of aluminum foam can reflect mechanical behavior in the compression process and good numerical results show that present method is applicable.

© 2013 Elsevier B.V. All rights reserved.

## 1. Introduction

Metal foams is an ideal lightweight structural material with many outstanding characteristics which makes it widely used in many industries, such as lightweight structures, energy absorption, thermal and acoustic management. Many scholars discussed the relationship of mechanical properties and heat transfer performance for metal foam with microstructure [1–7].

The research on compression performance of aluminum foam has focused on the factors which affect the compression behavior, such as the matrix material, the relative density, pore size, strain rate, micro-defects. Beals and Thompson [8] tested the compression performance of aluminum foam with the uneven density gradient, and then compared the results with that of the theoretical predicted by Gibson–Ashby model. The calculation results showed that the density gradient had a greater impact on compression performance. Nieh [9] illustrated that the mechanical strength and energy absorption characteristics would not be influenced by the pore size.

The mechanical properties of aluminum foam not only depend on the matrix material, but are also closely related to the pore structure. There are many shortcomings in the aluminum foam manufacturing process, for example, uneven pore structure, the

poor reproducibility of the preparation process. Therefore, many scholars used the finite element model (FEM) to research the relationship between the internal microstructure, and its mechanical properties through establishing various simplifying models. Gent and Thomas [10,11] first proposed the elastic spider network model and the cube structure model; they predicted the elastic modulus of the open-cell foam material and simulated stress–strain of foam materials, proved the elastic modulus of the foam material was proportional to relative density at low density. Pore element and structural element of Gibson–Ashby model [12] were both achieved structurally symmetrical and three-dimensional isotropic. However, due to inaccurate element-intensive, the equivalency of the prismatic structure and the stress of prism, there were various errors in the application process. Warren and Kraynik [13] used tetrahedral pillar structure model to discuss the elastic properties of three-dimensional open-cell foams. The results showed that the pillar bending was the main deformation mechanism of foam materials which had tetrahedron microstructure, and also obtained the relationship between the elastic modulus and the relative density when shape of the interface of pillar was circular cross-section, triangular cross-section and plateau section. Warren and Kraynik [14] also used the same method to discuss the cubo-octahedron model of the open-cell foam material on the basis of tetrahedral pillar model. The relationship of bulk modulus and shear modulus with micro-structure parameters was obtained. The microscopic structure parameters in the model included the length of the pillar, the axial elastic flexibility and

\* Corresponding author.

E-mail address: [zhuxiaolei856028@126.com](mailto:zhuxiaolei856028@126.com) (X. Zhu).

bending flexibility. Van Den Burg et al. [15] used the regular distribution of seed to establish Voronoi model of open-cell foam material based on the regular cell structure, which has been widely used. Three special seed distributions (body-centered cubic, face-centered cubic and nearly hexagonal) were selected by Van Den Burg to establish each Voronoi open-cell foam metal structure model. The Voronoi model was similar to the real foaming preparation process in the generation of the internal cell structure. Therefore, Voronoi model can be used to simulate the internal structure of the foam materials, however, there will be a great error in the calculation results by these simplified models when there is a hole through the matrix or the thickness of the pores wall is uneven.

In this paper, a novel modeling approach is proposed to establish the FEM for aluminum foam based on the MATLAB image processing technology and X-ray computed tomography ( $\mu$ CT) scanning technology. The method is aimed to obtain accurately calculation results by reconstructing geometrical model for real aluminum foam. This approach is applied to calculate the compression performance of aluminum foam. Their porosity was 56.41%, 56.71% and 58.02%, respectively; and the matrix material was ZL102.

**2. Methods**

*2.1. Geometric model*

When the  $\mu$ CT is used to scan the aluminum foam, the external environment, devices themselves and the distortion of the image format in conversion process will lead to the blurred image of edges. In order to extract useful information from the image, it must be pre-processed. The MATLAB is used to deal with  $\mu$ CT scanning image of aluminum foam and establish FEM model. The process is shown in Fig. 1.

*2.1.1. Binarization processing*

During the image processing, binary image processing is used to improve the efficiency of the image intensifier and contour extraction. The binary image processing for  $\mu$ CT scanning image of aluminum foam is partitioned into matrix and holes. As there is a great difference between the matrix and holes in the gray-scale, the threshold segmentation is used to separate matrix from the image. Then the determining of the threshold is the most important in present problem. There are several methods to determine the threshold, such as histogram troughs law, OTSU segmentation method, and maximum entropy method and so on.

Maximum entropy was firstly proposed by Pun [16]. The purpose is to divide the gray-level histogram of image into

separate classes and make maximum total entropy of all kinds of classes.

Consider “S” as potential segmentation threshold point, and  $p_0, p_1, p_2, \dots, p_L$  the gray levels. Two probability distributions are considered at the gray level “S”. A represents the foreground. B represents the background, and then

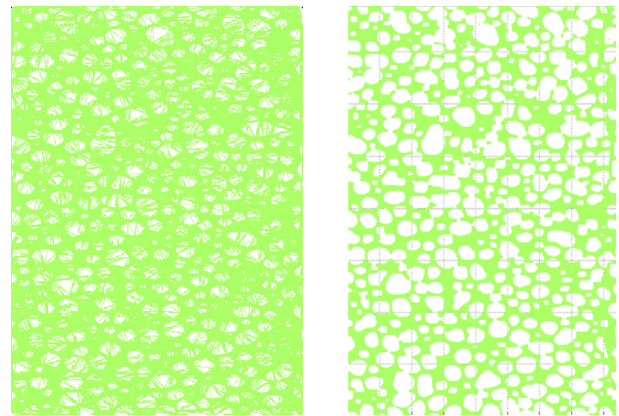
$$A : p_0/p_d, p_1/p_d, p_2/p_d, \dots, p_S/p_d \tag{1}$$

$$B : p_{S+1}/(1 - p_d), p_{S+2}/(1 - p_d), \dots, p_L/(1 - p_d) \tag{2}$$

where  $p_d = \sum_{i=0}^S p_i$ , L is the number of gray levels. Then, the entropy after segmentation image is calculated by Eq. (3).

$$H(S) = E_A + E_B \tag{3}$$

$$E_A = -\sum_{i=0}^S (p_i/p_d) \log(p_i/p_d) \tag{4}$$



(a) Global subdivision (b) Subdivision with constraint

Fig. 2. Delaunay triangle subdivision of aluminum foam materials.

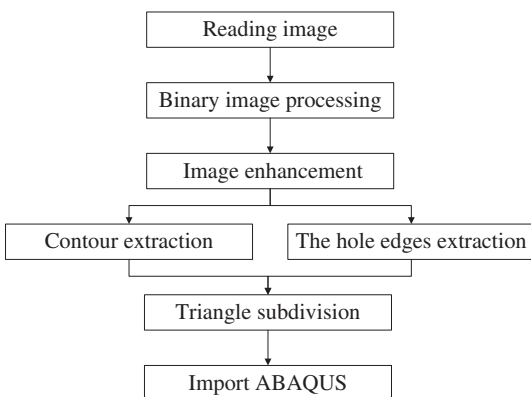


Fig. 1. Finite element modeling process based on MATLAB image processing.

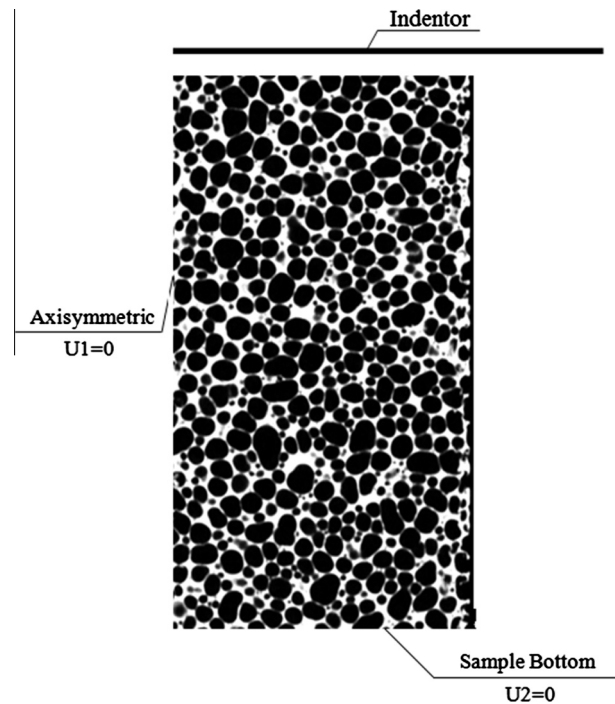


Fig. 3. The compression FEM and boundary condition of aluminum foam materials.

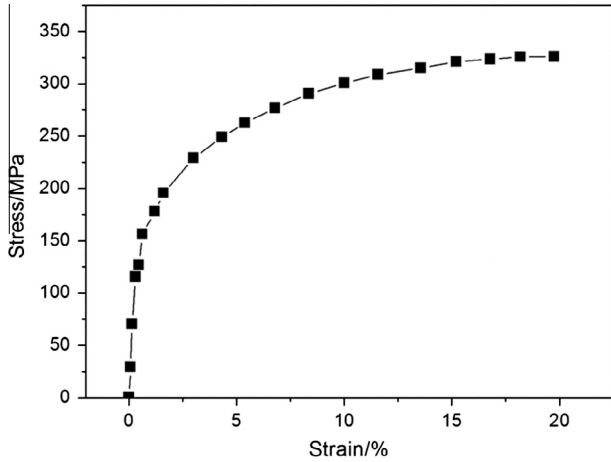


Fig. 4. Stress-strain of ZL102.

$$E_B = - \sum_{i=S+1}^L [p_i / (1 - p_d)] \log [p_i / (1 - p_d)] \quad (5)$$

When the entropy of image,  $H_0$  exists maximum, the best threshold value of image segmentation is shown in Eq. (6)

$$H_0 = \arg \max_S (H(S)) \quad (6)$$

If the exponential entropy,  $H_N$ , is adopted, the entropy after segmentation image can be obtained in Eq. (7) from Eq. (3),

$$H_N(S) = \sum_{i=0}^S \frac{p_i}{p_d} e^{1 - \frac{p_i}{p_d}} + \sum_{i=S+1}^L \frac{p_i}{1 - p_d} e^{1 - \frac{p_i}{1 - p_d}} \quad (7)$$

Then, the optimal threshold value of divided images is shown in Eq. (8),

$$H_0 = \arg \max_S (H_N(S)) \quad (8)$$

$H_0$  exists maximum when the gray level equal to  $S$ , then the  $S$  is the threshed value. The matrix and holes in the  $\mu$ CT scanning image is successfully differentiated by using the maximum entropy algorithm.

### 2.1.2. Image enhancement

Image enhancement is an operation to remove noise and high-light useful information. Usually, the noise is divided into external noise and internal noise. The external noises come from the outside of the processing system, such as electromagnetic interference. Internal noise has four common forms: (1) the noise caused by the basic of light and electricity; (2) the noise generated by the mechanical motion; (3) the noise caused by the defects of material themselves; and (4) the noise from the system of internal circuit. For the  $\mu$ CT scanning image of aluminum foam, the noise is mainly caused by the basic properties of light and electricity, and this noise may be enhanced after image binarization processing, the features mainly for the “salt & pepper” noise. For this type of noise, the median filtering algorithm is very effective.

### 2.1.3. Boundary extraction

The extraction of external contour and internal boundary is an important step to reconstruct geometric model of aluminum foam. The image edge detection is usually done by the first order or second order derivative. The common edge detection operator in MATLAB is Robert gradient operator, Sobel operator, Prewitt operator, Laplacian and so on. For aluminum foam, the “edge” function, which is provided by the MATLAB, is applied to detect the boundaries of aluminum foam matrix through constructing Prewitt operator. Then, the coordinate information of all the pixels on the boundary and internal is obtained.

### 2.1.4. Mesh

The traditional approach is to import those coordinates of pixels into reverse engineering software (such as Geomagic Studio, Image, PRO/E), reconstruct geometrical model by lofting, surface fitting and some other ways. Due to a lot of holes internal of aluminum foam and random distribution, there is a great difference between the actual model and the reconstructed geometric model by using reverse engineering, which makes the calculation results unsatisfactory.

In order to obtain effective calculation results based on porous structures of aluminum foam, more efficient meshing algorithm is needed. In this paper, the triangulation method is applied to mesh the aluminum foam directly. Two-step node filtration method is used to mesh this geometric model with island features. First step,

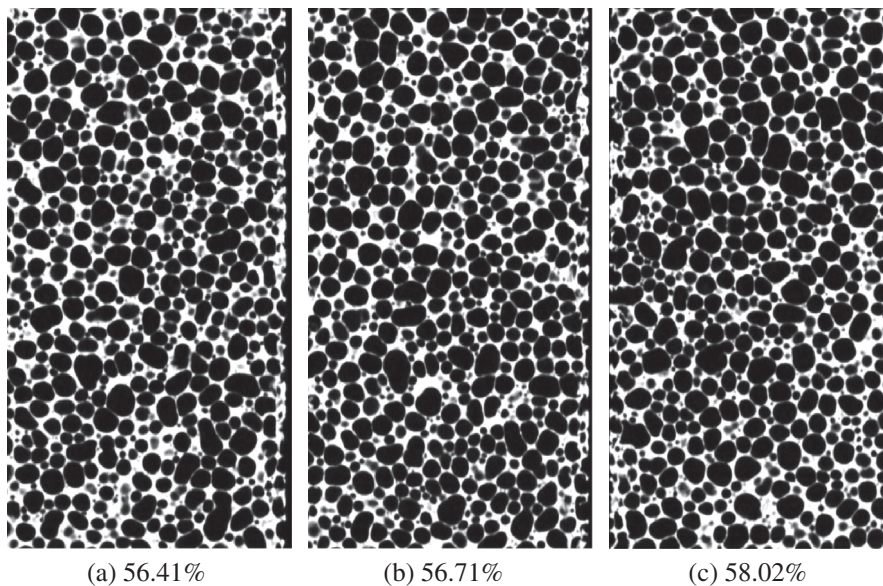


Fig. 5. The original image of aluminum foam materials.

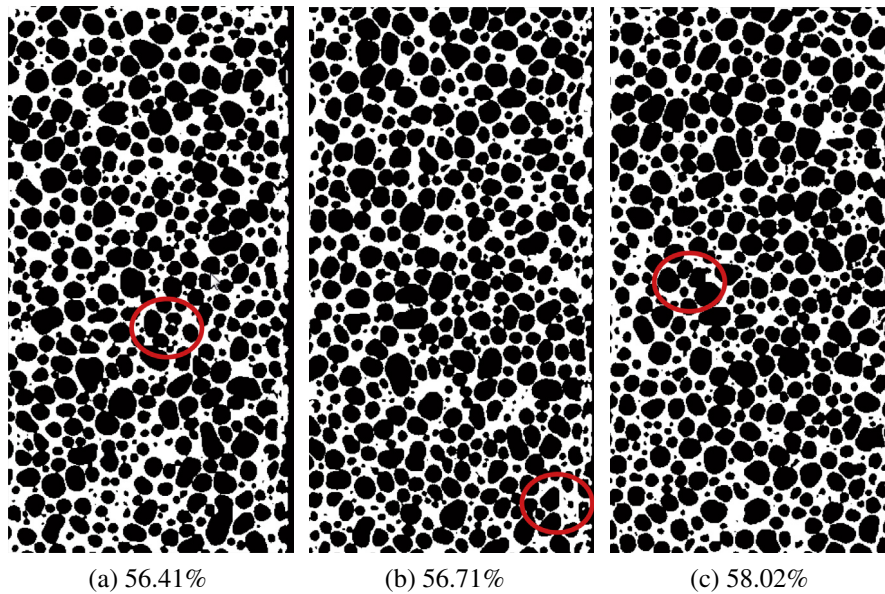


Fig. 6. Binarization image.

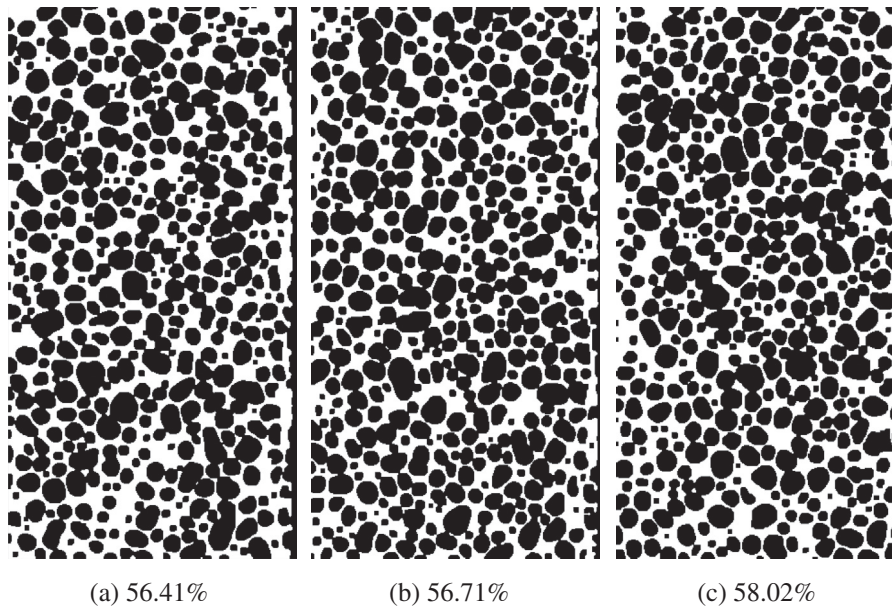


Fig. 7. Images after median filtering.

global was meshed by Delaunay triangulation. Second step, point-by-point filtering method is used to delete the triangular mesh with 3 internal boundary points. Then, the Delaunay triangulation of aluminum foam is obtained. It is worth to note that the pixels on the boundary must be chosen as the node, and the interval take point method is used to pick up the node of matrix in the premise of guaranteeing the minimal difference between geometric model and the real one. The comparison results are shown in Fig. 2.

In conclusion, FEM is established by the direct method, selecting node from all of pixels directly, and then meshing them. In this way, there is a smaller difference in structure size between the geometric model and the real one; a lot of computer resources can be saved and the computational efficiency can be improved

by controlling the number of the nodes on the premise of guaranteeing authenticity.

## 2.2. Boundary condition

The boundary condition of aluminum foam compression FEM is shown in Fig. 3. The indenter is rigid body, contacting with the upper surface of the specimen in the process of compressed. The frictionless contact boundary condition is used. The axis symmetry plane and the bottom surface of the specimen are all applied with displacement boundary as shown in Fig. 3. The element type is CAX3. Material is ZL102 with Young's modulus, Poisson ratio and yield strength 70 GPa, 0.33 and 120 MPa, respectively [17]. The stress-strain curve is shown in Fig. 4.

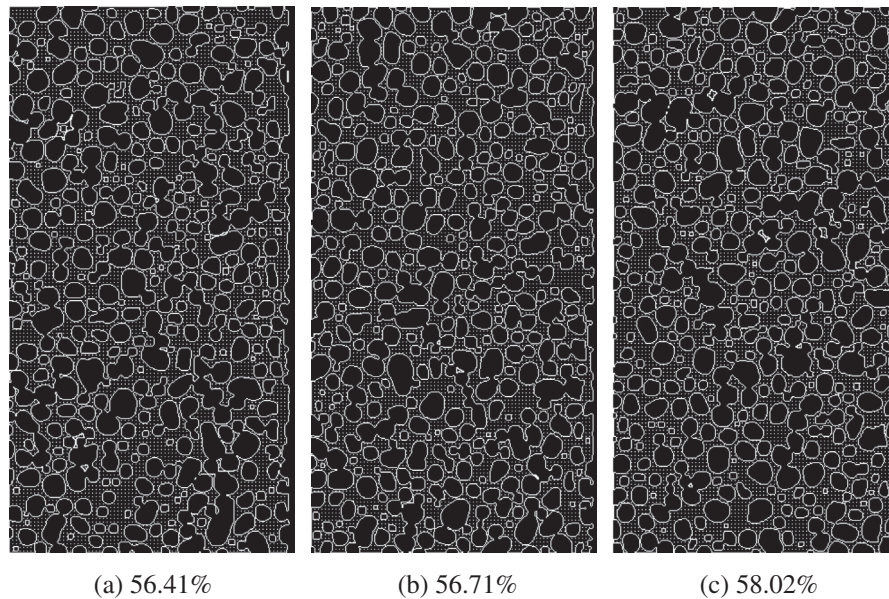


Fig. 8. Node distribution.

### 3. Numerical example

The aluminum foam reconstruction algorithm based on MATLAB image process is applied to rebuild aluminum foam and calculate its compression performance, when porosity is 56.41%, 56.71% and 58.02%, respectively. The original  $\mu$ CT scanning images are shown in Fig. 5.

The aluminum foam binarization was implemented by using the maximum entropy algorithm. The results are shown in Fig. 6. A small amount of “salt & pepper” noise exist in the image after binarization, and some cusps on the boundary of the holes has a difference with those on the original image, therefore, median filtering is conducted and the results are shown in Fig. 7.

On the premise of guaranteeing the minimal difference between reconstruction geometrical model and real one, the pixels on the boundary must be chosen as the node, and the interval take point method is used to pick up the node of matrix, of which the results are shown in Fig. 8. The two-step method is applied to triangulation of aluminum foam with island features, and the mesh are shown in Fig. 9.

Finally, the node coordinates information and element information are written into the INP file, and imported into the ABAQUS to calculate the result. The stress distribution is obtained when the compression amount is 10 mm, which is shown in Fig. 10. The relationship of compression displacement with the loads is shown in Fig. 11.

As shown in Fig. 10, only local holes collapse when the amount of compression is 10 mm, and the collapsed positions in three examples are different. It illustrates that calculation is independent on geometric modeling algorithm. As it is known, the compression of aluminum foam material is divided into three stages: linear elastic stage, plastic platform stage and densification stage. When the deformation is small, load and displacement relation is linear, and this stage is very short which mainly reflect the strength characteristics of pore structure. Then a longer plastic yielding platform appears with the compressive deformation increasing. Load is almost the same as the increase of the deformation, and this stage mainly reflects the walls of the pores are crushed. Finally, all holes are crushed, and the walls of the pores squeeze together. The aluminum foam material is compacted, and the stress will increase

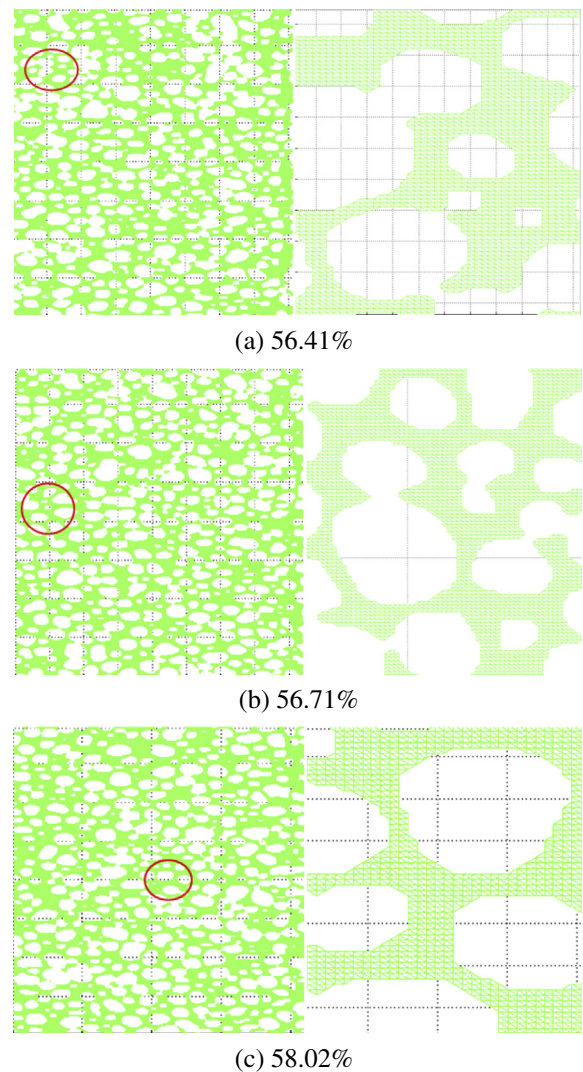
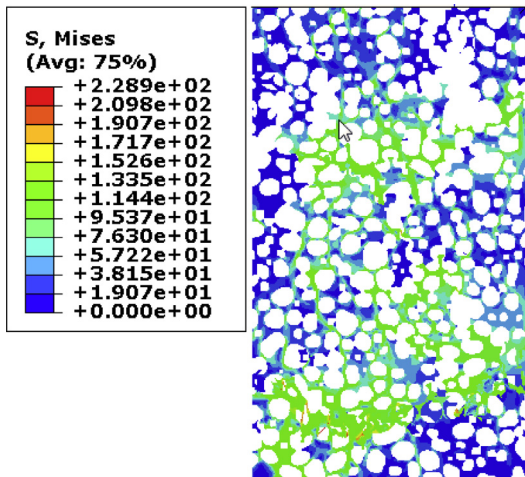
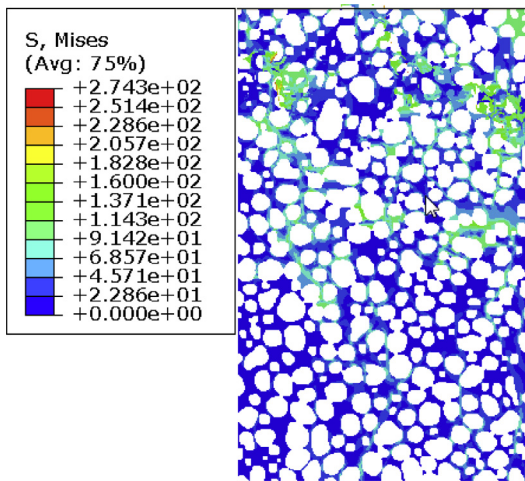


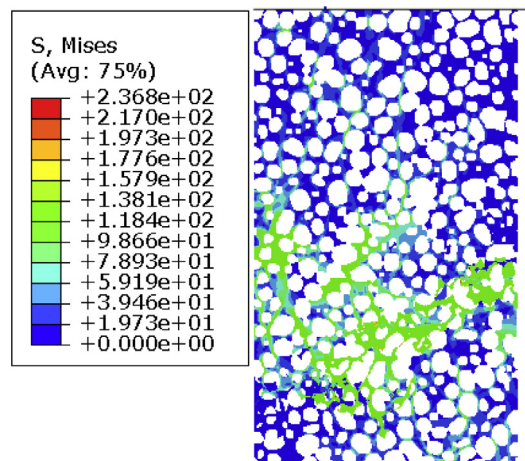
Fig. 9. Mesh image.



(a) 56.41%



(b) 56.71%



(c) 58.02%

Fig. 10. The stress distribution of amount of compression equal to 10 mm.

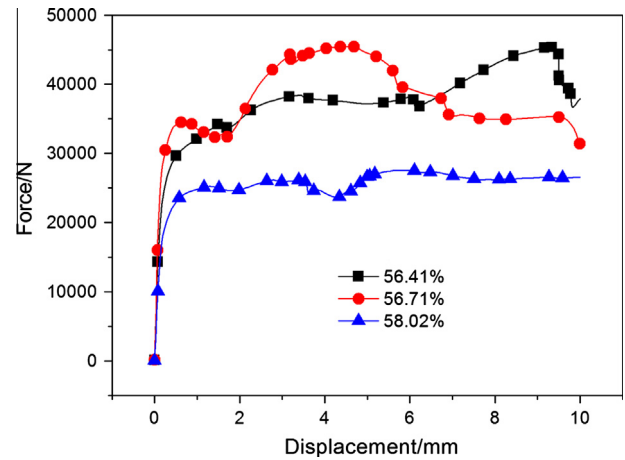


Fig. 11. The relationship between load and the compressive displacement.

into the plastic stage of platform, the load is changed in a certain range with displacement increasing, and the change range is smaller at porosity equal to 58.02%. The above numerical examples illustrate that it can simulate well the mechanical behavior of the aluminum foam, which prove that the novel modeling approach of aluminum foam is applicable.

#### 4. Conclusions

In this paper, a new modeling approach which can be applied in modeling of foam material is proposed. First of all, MATLAB software is used to deal with  $\mu$ CT scanning images of real aluminum foam material. Secondly, the two-step mesh method is employed to discrete network by appropriate selection of node. And then establish the FEM of aluminum foam material directly. This approach is used to calculate the compression performance of aluminum foam, whose porosity is equal to 56.41%, 56.71% and 58.02%, respectively. The calculation of aluminum foam can reflect mechanical behavior in the compression process and good numerical results show that present method is applicable.

#### References

- [1] F.S. Han, Z.G. Zhu, *Journal Materials Science* 34 (1999) 291–298.
- [2] J.A. Ramin, M. Zahrani, N. Behzad, *Materials and Design* 51 (2013) 1035–1044.
- [3] X.C. Xia, H. Feng, X. Zhang, W.M. Zhao, *Materials and Design* 51 (2013) 797–802.
- [4] C.H. Yang, Y. An, M. Tort, P.D. Hodgson, *Computational Materials Science* 81 (2013) 89–97.
- [5] T. Fiedler, C. Veyhl, I.V. Belova, T. Bernthaler, B. Herne, G.E. Murch, *Computational Materials Science* 74 (2013) 143–147.
- [6] T. Fiedler, I.V. Belova, G.E. Murch, *Computational Materials Science* 50 (2010) 503–509.
- [7] K.K. Bodla, J.Y. Murthy, S.V. Garimella, *Computational Materials Science* 50 (2010) 622–632.
- [8] J.T. Beals, M.S. Thompson, *Journal of Materials Science* 32 (1997) 3595–3600.
- [9] Hidetaka Kanahashi, Toshiji Mukai, T.G. Nieh, Tatsuhiro Aizawa, Kenji Higashi, *Materials Transactions* 43 (2002) 2548–2553.
- [10] A.N. Gent, A.G. Thomas, *Journal of Applied Polymer Science* 1 (1959) 107–113.
- [11] A.N. Gent, A.G. Thomas, *Rubber Chemistry Technology* 36 (1963) 597–610.
- [12] L.J. Gibson, M.F. Ashby, *Cellular Solids: Structures and Properties*, Cambridge University Press, United Kingdom, 1997.
- [13] W.E. Warren, A.M. Kraynik, *Journal of Applied Mechanics* 55 (1988) 341–346.
- [14] W.E. Warren, A.M. Kraynik, *Journal of Applied Mechanics* 64 (1997) 787–794.
- [15] M.W.D. Van der Burg, V. Shulmeister, E. Van der Giessen, R. Marissen, *Journal of Cellular Plastics* 33 (1997) 31–54.
- [16] T. Pun, *Signal Processing* 2 (1980) 223–237.
- [17] Y.H. Yu, Z. Yang, B. Liang, *Computer Simulation* 27 (2010) 317–341 (in Chinese).

rapidly. As shown in Fig. 11, when the amount of compression displacement increases from 0 mm to 10 mm, a short elastic stage appears with the amount of deformation is 0.5 mm. Then entering